IOPscience iopscience.iop.org

Home Search Collections Journals About Contact us My IOPscience

Defect generation in high κ gate dielectric stacks under electrical stress: the impact of hydrogen

This article has been downloaded from IOPscience. Please scroll down to see the full text article.

2005 J. Phys.: Condens. Matter 17 S2075

(http://iopscience.iop.org/0953-8984/17/21/004)

View the table of contents for this issue, or go to the journal homepage for more

Download details:
IP Address: 129.252.86.83
The article was downloaded on 28/05/2010 at 04:52

Please note that terms and conditions apply.

INSTITUTE OF PHYSICS PUBLISHING JOURNAL OF PHYSICS: CONDENSED MATTER

J. Phys.: Condens. Matter **17** (2005) S2075–S2088 doi:10.1088/0953-8984/17/21/004

Defect generation in high κ gate dielectric stacks under electrical stress: the impact of hydrogen

M Houssa[1], G Pourtois[1], M M Heyns[1] and A Stesmans[2]

[1] IMEC, 75 Kapeldreef, B-3001 Leuven, Belgium
[2] Department of Physics, University of Leuven, Celestijnenlaan 200 D, B-3001 Leuven, Belgium

Received 6 December 2004, in final form 7 February 2005
Published 13 May 2005
Online at stacks.iop.org/JPhysCM/17/S2075

Abstract

The role of hydrogen on the generation of defects in high κ based devices, subjected to an electrical stress, is discussed, with an emphasis on issues related to negative bias temperature instabilities (NBTI) in SiO_2/HfO_2 based devices. It is shown that NBTI are mainly caused by the buildup of positively charged defects in the gate stack. The defect density is found to increase with the forming gas annealing temperature of the device. The defects are robust under electron injection from the Si substrate, but they can be partly removed by annealing the devices in N_2 at 200 °C. All these results suggest that protons are most probably involved in the positive charge buildup. A kinetic model is proposed, based on the dispersive transport of protons in the gate stack during the electrical stressing, followed by their trapping in the HfO_2 layer, forming hydrogen-induced overcoordinated oxygen centres. *Ab initio* calculations further indicate that the protons are stabilized in monoclinic HfO_2 by forming bonds with trivalent oxygen centres, and that these defects are not producing any energetic level in the HfO_2 band gap. The kinetic model allows one to explain most of the observed experimental data, i.e. the time and voltage dependence of the positive charge buildup, the dependence of the positive charge density on the forming gas annealing temperature, as well as its robustness versus electron injection from the Si substrate.

(Some figures in this article are in colour only in the electronic version)

1. Introduction

Hydrogen plays a crucial role in many technological processes used in the semiconductor industry [1]. For example, it is well known that hydrogen can efficiently passivate one of the most important defects in metal–oxide–semiconductor field effect transistors (MOSFETs), namely Si trivalent dangling bonds at the (100)Si/SiO_2 interface, so-called P_{b0} [2, 3]. On the other hand, hydrogen can also be detrimental to the device properties. For example, hydrogen

 © 2005 IOP Publishing Ltd Printed in the UK

related defects, present in the gate dielectric layer, can act as carrier trapping centres when the device is subjected to an electrical stress [4] or exposed to ionizing irradiation [5–7], resulting in device degradation and, ultimately, to the gate dielectric breakdown. Exposure of SiO_2 layers to high temperature hydrogen-containing ambient is also known to produce positive charges, most probably hydrogen-induced overcoordinated defects [8, 9].

High κ gate dielectrics are currently under investigation for the replacement of SiO_2 gate insulator in the future generations of MOSFETs [10]. One of the major reasons is that the leakage current flowing through SiO_2 layers thinner than 1 nm exceeds 100 A cm^{-2} at operating voltage (around 1 V), leading to unacceptable power dissipation in the circuits. For a given technology, determined e.g. by the transistor gate length and equivalent electrical thickness of the gate insulator, the use of high κ gate dielectrics would allow us to use physically thicker layers, aiming at reducing the leakage current flowing through the devices. In that respect, ZrO_2 and HfO_2 are considered as viable high κ gate dielectric candidates, due to their high dielectric constant (about 20), good thermal stability, allowing them to sustain the high thermal budgets required for the fabrication of advanced MOS devices, and sufficiently high value of the Si/ZrO_2 and Si/HfO_2 conduction and valence band offsets [10].

In previous works, we have pointed out the role of hydrogen in the degradation of the electrical properties of high κ gate dielectric stacks under electrical stress, e.g. interface state generation under constant voltage stress [11, 12], stress-induced leakage current [13, 14] and positive charge generation [14, 15]. The present work is focused on the impact of hydrogen on one of the most important reliability issues in advanced MOS devices: negative bias temperature instabilities (NBTI).

NBTI occurs in p-channel MOSFETs under inversion conditions. Let us consider the simple example of a complementary MOS inverter, schematically illustrated in figure 1(a). When the p-channel transistor is turned on at elevated temperature (typically between 100 and 150 °C), i.e. when the gate is negatively biased with respect to the substrate, defects are generated in the device, resulting in threshold voltage (V_{th}) shifts and reduction of the drive current (I_{dsat}) of the devices, as illustrated in figure 1(b). The degradation of these device parameters can then lead to the failure of integrated circuits, both for analogue and digital applications [16].

In SiO_2 based devices, the most important defects involved in NBTI are supposed to be P_{b0} centres [17–19]. During the negative bias temperature (NBT) stressing, holes attracted at the Si/SiO_2 interface can induce the depassivation of P_{b0} centres (initially passivated by hydrogen during the forming gas annealing of the device), followed by the diffusion of hydrogen species away from the interface, the rate limiting step for P_{b0} centre generation being the diffusion process [18, 19]. This is the so-called reaction–diffusion model of NBTI, which can explain the time, temperature and oxide electric field (E_{ox}) dependence of V_{th} shifts in SiO_2 based devices, which can be phenomenologically described by the expression

$$\Delta V_{th} \approx C E_{ox}^{m} \exp\left(\frac{-E_a}{k_B T}\right) t^{\alpha} \tag{1}$$

where C is a constant, $m \sim 3$–4, $E_a \sim 0.1$–0.2 eV and $\alpha \sim 0.2$–0.25.

So far, not much work on NBTI in high κ gate dielectrics has been reported in the literature [20–22]. In this work, we study in detail the V_{th} shifts observed in poly-Si/HfO_2 based pMOSFETs under NBT stress, and more specifically discuss the possible role of hydrogen species (protons) in device degradation.

The paper is organized as follows. The device fabrication process is described in section 2. The experimental results are presented in section 3, and *ab initio* calculations on the stability of protons in monoclinic HfO_2 are discussed in section 4. A kinetic model, based on the

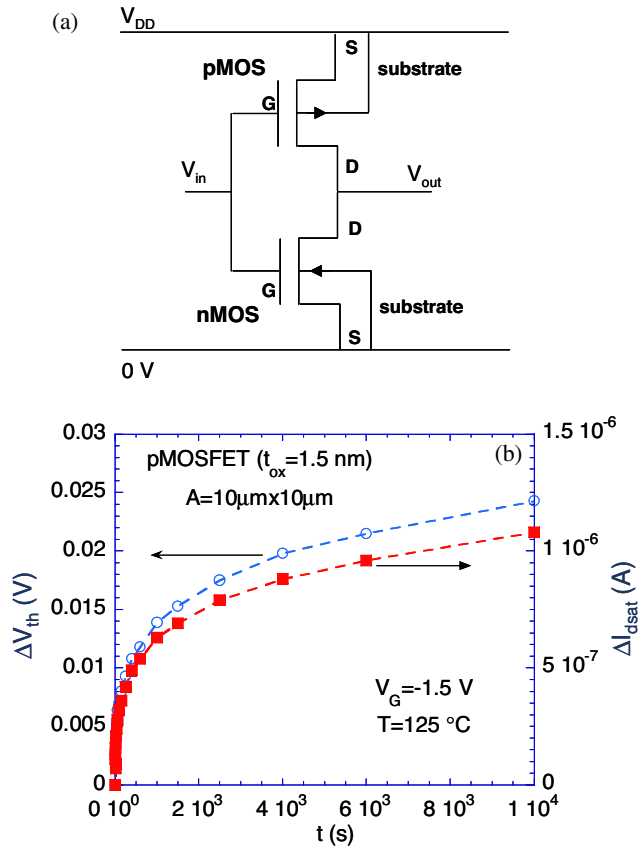

Figure 1. (a) Schematic diagram of a complementary MOS inverter. (b) Threshold voltage (open circles) and drive current (filled squares) shifts of a pMOSFET, with a 1.5 nm SiON layer, as a function of time.

dispersive transport of protons and their trapping in the HfO_2 layer, is presented in section 5. Conclusions are finally drawn in section 6.

2. Experimental details

p-channel MOSFETs were fabricated using a conventional self-aligned transistor flow. Prior to HfO_2 deposition, a chemical silicon oxide layer (O_3 based chemistry) of about 1 nm was grown on the Si substrate. HfO_2 was deposited by atomic layer deposition (ALD) in an ASM Pulsar 2000 reactor using $HfCl_4$ and H_2O as sources. The thickness of the HfO_2 layer was estimated from high resolution cross-sectional transmission electron microscopy (HRTEM) to be 4 nm. A typical HRTEM picture of a SiO_2/HfO_2 stack is shown in figure 2(a). The gate stack was next annealed in dry O_2 at 500 °C for 1 min. p^+ poly-Si gates (boron doped) were then patterned on the gate stack. The dopants were activated at 1000 °C (spike anneal) in 5% O_2. The devices were finally exposed to a forming gas anneal (FGA, 10% H_2/90% N_2) at 520 or 580 °C for 20 min, ensuring an efficient passivation of interface defects [23, 24]. The equivalent oxide thickness of the stack was estimated to be 1.8 nm from the analysis of the capacitance–voltage characteristics of the devices.

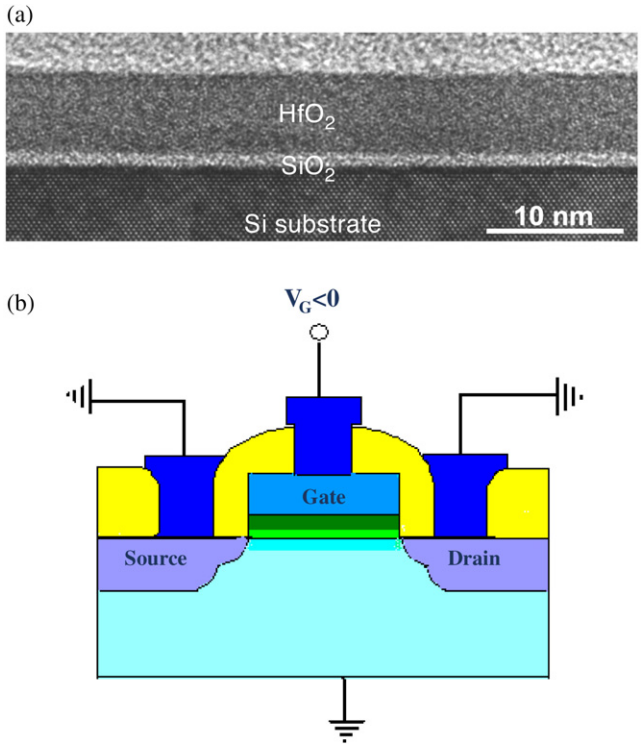

Figure 2. (a) High resolution cross-sectional transmission electron microscope image of a 1 nm SiO_2/4 nm HfO_2 stack. (b) Schematic diagram of a pMOSFET under negative bias temperature stress.

NBT stressing was carried out at different temperatures, ranging from 75 to 150 °C, with a constant negative gate bias, and with source, drain and substrate grounded, as illustrated in figure 2(b). The threshold voltage of the device was recorded periodically during the stressing by measuring its drain current–gate voltage characteristics at a fixed drain voltage of −100 mV, using a HP4156C semiconductor parameter analyser.

3. Results and discussion

The shifts of the drain current I_D—gate voltage V_G characteristics of a pMOSFET with a SiO_2/HfO_2 stack (exposed to FGA at 580 °C), stressed at −1.5 V and 125 °C for different times, are shown in figure 3(a). One observes that the threshold voltage, V_{th}, of the device is shifting to a more negative value after NBT stressing, indicating the buildup of positive charges. The measured time dependence of the threshold voltage shift, $\Delta V_{th} = IV_{th}(t) - V_{th}(0)I$, of pMOSFETs is shown in figure 3(b), for different values of the gate voltage stress. One observes that ΔV_{th} increases quickly and reaches a saturation value of about 90 mV. This behaviour is markedly different from the one observed for SiO_2 based devices, where ΔV_{th} saturation is not usually observed for stress time up to about 5×10^4 s, and indicates the buildup of positively charged defects in the gate stack. One can also note the absence of a significant stretching of the I_D–V_G characteristics after NBT stressing, unlike in SiO_2 based devices [25], indicating negligible interface state generation.

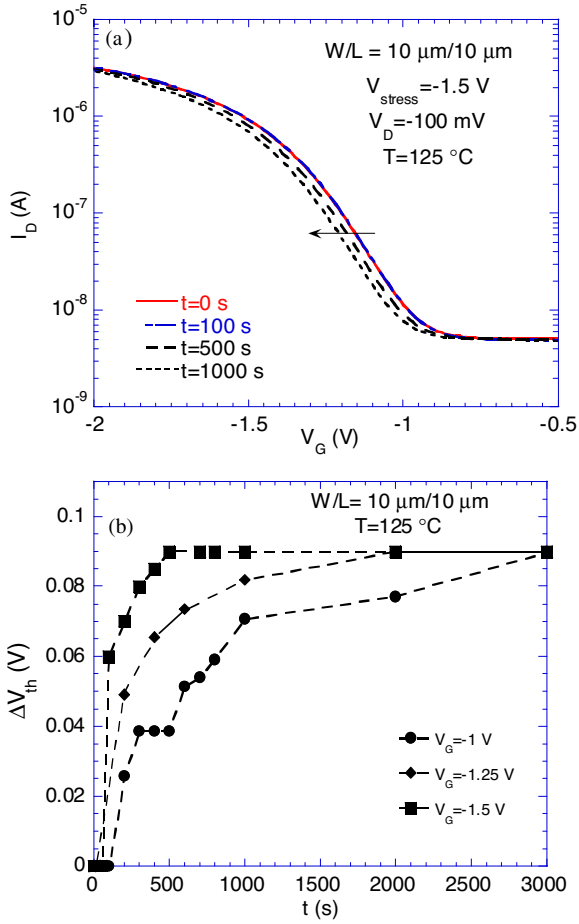

Figure 3. (a) Drain current I_D—gate voltage V_G characteristics of a pMOSFET measured periodically during NBT stressing at −1.5 V and 125 °C. (b) Threshold voltage shifts of pMOSFETs as a function of stressing time, for devices under NBT stress at different gate voltages.

The effective density of positive charge, N_{ox}, generated during NBT stressing at −1.5 V is shown in figure 4 as a function of the stress time, for devices annealed in FGA at 520 (open symbols) and 580 °C (filled symbols). N_{ox} was estimated from the V_{th} shifts according to the expression [26]

$$N_{ox} = \frac{C_{ox}\Delta V_{th}}{q} \tag{2}$$

where C_{ox} is the gate stack capacitance per unit area and q the electron charge. One observes that the charge buildup is faster and the saturation value is enhanced by a factor of about 2 in devices that received the higher FGA temperature, suggesting that hydrogen is involved in device degradation.

The annealing behaviour of the positive charge is illustrated in figure 5. A device exposed to 580 °C FGA was first subjected to NBT stress at −1.5 V for 2000 s. The threshold voltage was next periodically measured after annealing the transistor in N_2 at a fixed temperature. As shown in figure 5, the positive charge density can be partly removed at 200 °C, but is not altered at 125 °C.

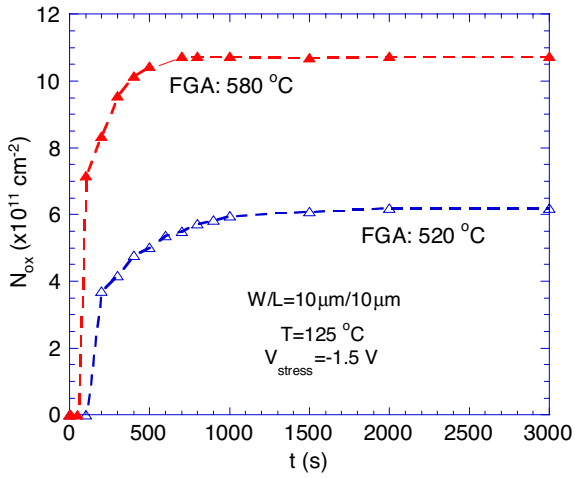

Figure 4. Effective density of positively charged defects, N_{ox}, as a function of time of pMOSFET exposure to NBT stress at −1.5 V and 125 °C. Open and filled symbols correspond to devices exposed to FGA at 520 and 580 °C, respectively.

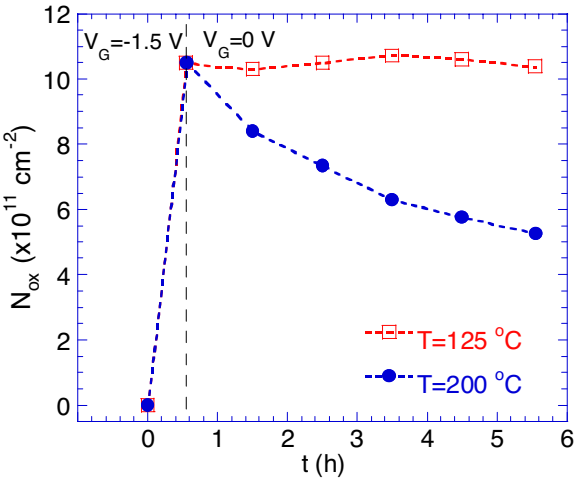

Figure 5. Effective density of positively charged defects as a function of time for pMOSFETs, first subjected to a NBT stress at −1.5 V for 2000 s, and next annealed in N_2 at 125 or 200 °C.

The possible neutralization of the positive charge by electron injection was next investigated. After NBT stressing at −1.5 V for 2000 s, a positive gate bias fixed at +1 V was applied to the device in order to inject electrons in the gate stack from the Si substrate accumulation layer; the gate current density at +1 V is about 10^{-6} A cm^{-2}; cf figure 6(a). The threshold voltage was then measured periodically during the positive gate voltage stressing. As shown in figure 6(b), the positive charge is not neutralized by the subsequent electron injection. On the contrary, the V_{th} shift slightly increases after positive gate bias stressing, which could be due to the generation of P_{b0} centres induced by electron injection [11].

The partial annealing of the positive charge at 200 °C and its robustness versus electron injection are further indications that the positive charge is induced by hydrogen. As a matter

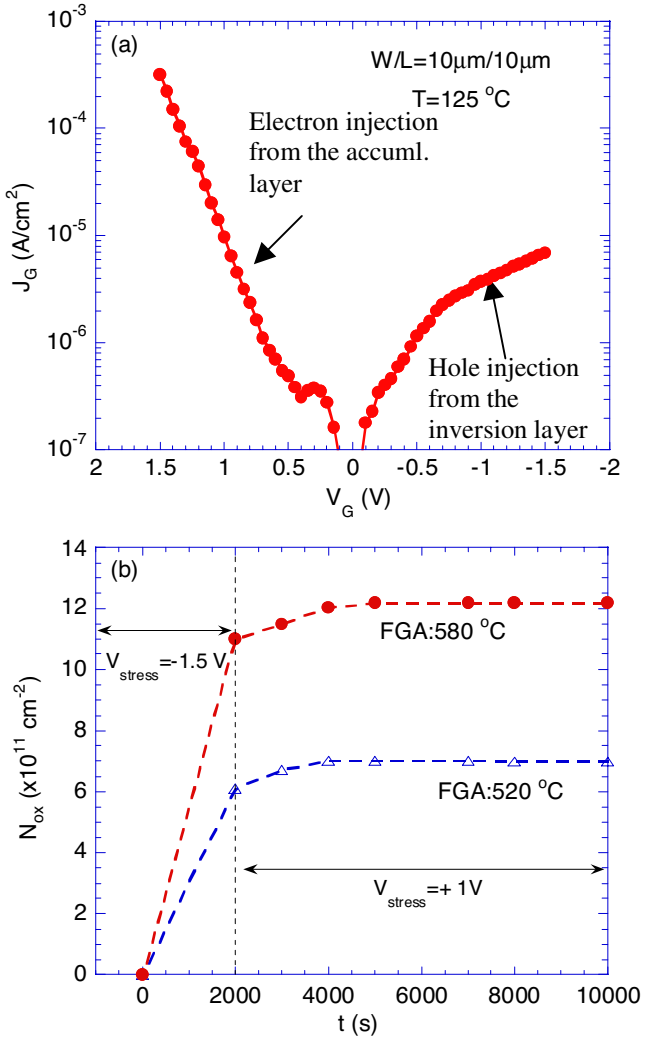

Figure 6. (a) Current–voltage characteristics of a pMOSFET at 125 °C, illustrating the tunnelling of electrons from the Si substrate accumulation layer under positive gate bias, and the tunnelling of holes from the Si substrate inversion layer under negative gate bias. (b) Effective density of positively charged defects as a function of time for pMOSFETs, first subjected to a NBT stress at −1.5 V for 2000 s, and next stressed under a positive gate bias at +1 V. Open and filled symbols correspond to devices exposed to FGA at 520 and 580 °C, respectively.

of fact, it has been suggested that hydrogen-induced overcoordinated oxygen centres in SiO_2, $[Si{=}O_2H]^+$, can be annealed at temperatures higher than 150 °C [27], but cannot be neutralized under electron injection, the energetic level of these defects residing in the SiO_2 conduction band [8, 28].

From these experimental results, the positive charge generation during NBT stressing can be explained as follows. When a negative voltage is applied to the gate, interstitial hydrogen atoms present close to the Si/SiO_2 interface donate their electrons to the Si substrate, forming protons. These protons will then be transported (dispersively) towards the gate, which is negatively biased. These protons can be subsequently trapped at bridging oxygen centres

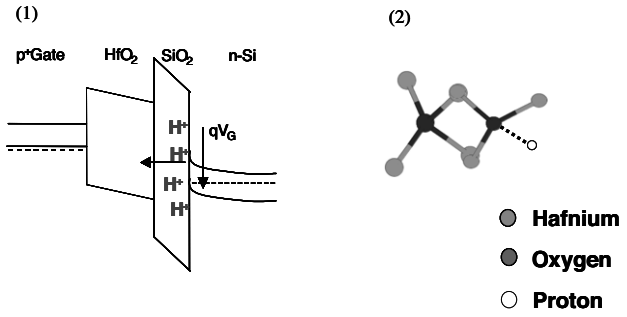

Figure 7. Schematic energy band diagram of an n-Si/SiO_2/HfO_2/p^+-Si structure, illustrating the dispersive transport of protons away from the Si/SiO_2 interface during NBT stressing (1), followed by their trapping at trivalent oxygen centres in the HfO_2 layer (2).

in the gate stack, forming overcoordinated positively charged centres [8, 9], as illustrated in figure 7. To verify this hypothesis, *ab initio* calculations of proton stability in monoclinic HfO_2 have been performed. These calculations are described in the next section.

4. Proton stability in monoclinic HfO_2

Ab initio calculations have been performed within the density functional theory (DFT), using spin-polarized DFT and the local density approximation (LDA). We used a numerical atomic approximation as it is implemented in the SIESTA code [29, 30]. Core electrons are implicitly treated by using Troullier–Martin pseudopotentials. The pseudopotentials were generated with the electronic configuration Hf [Xe $4f^{14}$]$5d^2 6s^2$, O[$1s^2$]$2s^2 2p^4$ and H $1s^1$, where the core configurations are shown in square brackets. The basis sets were of the DZP type: double ξ with polarization. The energy shifts, which determine the cut-off radii of the basis set wavefunctions, were around 200 meV. In order to validate both the basis set and pseudopotentials, the unit cell parameters were computed for monoclinic hafnium oxide. A good agreement between calculated and experimental structural parameters was found.

The defect calculations were made using a 96-atom unit cell, which is generated by extending the monoclinic unit cell by two in three dimensions. The monoclinic structure is used in the simulations since it is the most stable crystallographic phase [31]. A plane wave cut-off of 140 Ryd and four k points have been used, which ensures a convergence for this cell of 50 meV. The large size of the cell leads to a separation of $\sim$10 Å between the periodic images of the charged defects, which results in a Coulomb interaction energy that does not exceed $\sim$0.1 eV [32, 33]. During defect calculations, the cell has been considered as a part of an atomic reservoir, in which the lattice vectors are kept fixed, which corresponds to a very dilute system. All the atoms were allowed to relax until a 0.05 eV $Å^{-1}$ force tolerance was reached.

In the monoclinic HfO_2 crystal phase, the oxygen bridging sites are non-equivalent, adopting a trigonal or a tetragonal bridging coordination; see figure 8(a). During their transport towards the gate, the protons can hence interact on either one of the two coordination sites or be 'shared' between two bridging oxygen units, as illustrated in figure 8(b). To shed light on the most relevant overcoordination scenario, we introduced an interstitial proton in each of the different conformations. We then let the system relax to accommodate the presence of the proton and adopt an energetically stable structure. The minimization process leads, independently of the initial conformation, to the localization of the proton at the trivalent

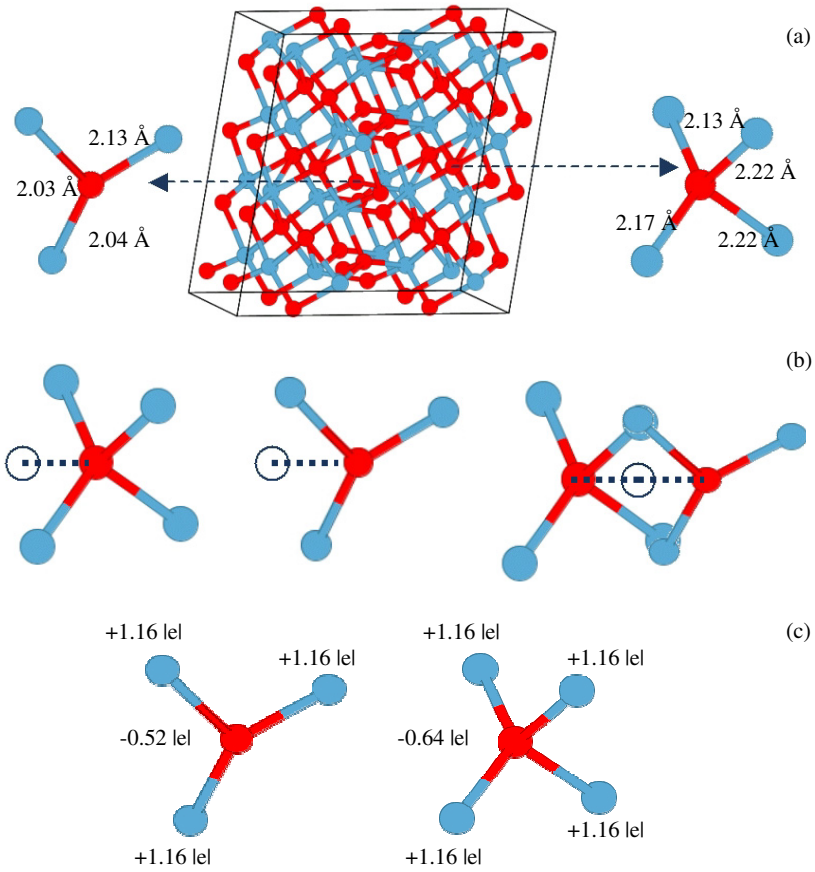

Figure 8. (a) Illustrations of the threefold-coordinated trigonal (left) and fourfold-coordinated tetragonal (right) oxygen atoms in monoclinic hafnia. (b) Illustration of the possible trapping sites for the proton in HfO_2. (c) Mülliken partial charges computed for the two coordination centres; a positive value corresponds to an electron density loss. In these schematic diagrams, oxygen, hafnium and hydrogen atoms are pictured as heavy grey, light grey and white circles, respectively.

oxygen centre. This suggests that these centres are the most stable trapping sites. Note that analogous studies [34, 35] involving oxygen interstitial incorporation in zirconia and hafnia have also found that there is no stable minimum for charged defects on tetravalent sites. Indeed, the tetravalent oxygen coordination generates (i) a spatial distribution of positively charged hafnium atoms that 'screens' the central oxygen atoms, as illustrated in figure 8(c), and (ii) a significant steric hindrance around the oxygen centre that prevents any proton overcoordination from occurring.

At a trigonal oxygen centre, the hafnium atoms take a quasi-planar configuration, which reduces both the Coulomb screening and the steric hindrance of the oxygen atom. This enables access for an out-of-plane proton interaction and results in the formation of a covalent H–O bond (whose length is close to the H–O bond length in water, i.e. about 0.96 Å). To accommodate the presence of the interstitial proton, the hafnium–oxygen bonds elongate slightly ($\sim$0.12 Å) and adopt lengths characteristic of a tetravalent oxygen centre.

The overcoordination of the oxygen bridging sites has little influence on the electronic structure of HfO_2. Indeed, the density of states of the protonated hafnium oxide, shown in

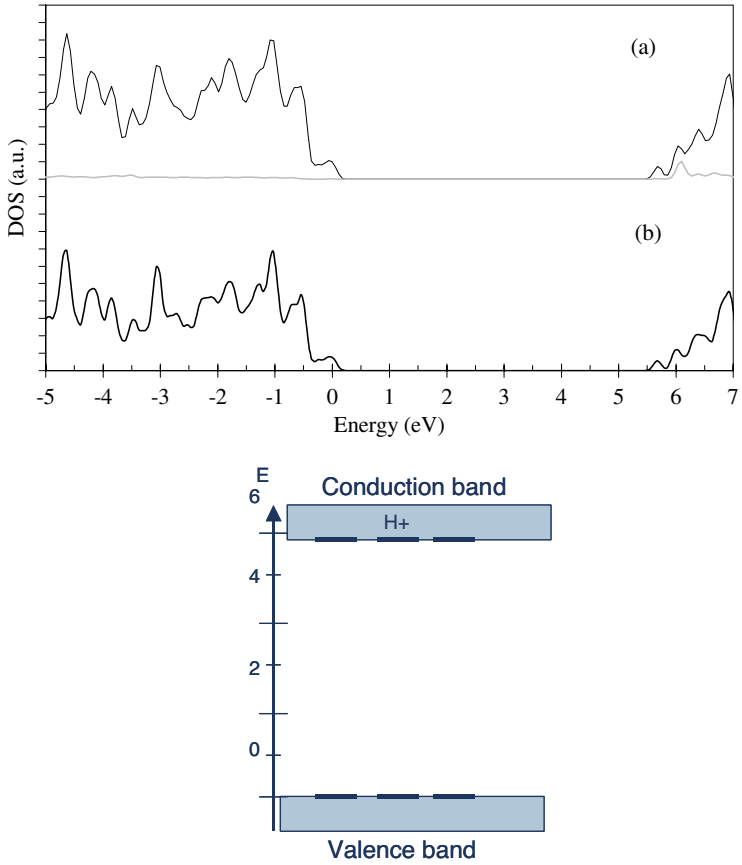

Figure 9. Total density of states (DOS) and partial density of states (PDOS) for protonated (a) and ideal (b) monoclinic hafnia, in arbitrary units. The PDOS of the trapped proton is shown in grey. A Gaussian smearing of 0.1 eV has been applied to the DOS. The conduction band states of HfO_2 have been rigidly shifted by 1.89 eV to account for the typical LDA underestimation of the electronic gap (3.79 eV) with respect to the experimental value (5.68 eV); see the bottom figure. The PDOS of the trapped proton has been magnified by 50 for reasons of clarity. The zero energy level is set at the top of the valence band.

figure 9, reveals that the electronic levels of the overcoordinated oxygen centre are located at the bottom of the conduction band, such that no defect states appear within the electronic band gap of HfO_2. This latter finding complies with the picture inferred from our NBTI experiments, in which the neutralization of the proton-induced positive charge by subsequent electron injection cannot occur, since the proton-induced defect electronic states lie above the HfO_2 band gap (and consequently, cannot be accessed by electrons injected from the Si substrate conduction band).

5. Kinetic model

On the basis of these DFT calculations, a kinetic model for the positive charge buildup is developed. It is assumed that interstitial protons present close to the Si/SiO_2 interface are transported dispersively [36–38] towards the gate during the NBT stressing, these protons being

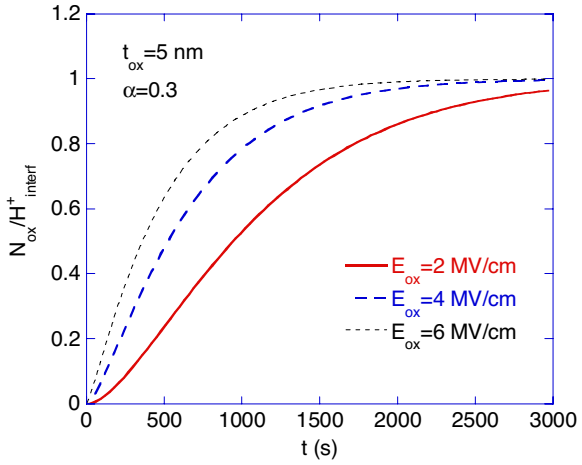

Figure 10. Calculated normalized density of positively charged defects, N_{ox}/H^+_{interf}, as a function of time, for different values of the oxide electric field E_{ox}.

subsequently trapped at trivalent oxygen centres in the HfO_2 layer, forming overcoordinated positively charged defects.

The dispersive transport of protons in the gate layer, e.g. the random hopping of H^+ from a bridging oxygen atom to the neighbour one, can be described by the expression [37]

$$[H^+] = [H^+_{interf}] \int_0^{t_{ox}/\mu t^\alpha} G(y)\,dy, \tag{3}$$

where $[H^+_{interf}]$ is the density of protons at the Si/SiO_2 interface, t_{ox} the gate stack thickness, $0 < \alpha < 1$ the dispersive transport exponent [37] and μ the average displacement per hop. The function $G(y)$ in equation (3), where $y = x/\mu t^\alpha$, is related to the probability $P(x, t)$ for finding a hopping ion at a distance x from the Si/SiO_2 interface at time t. The improved trial function described by McLean and Ausman [39] was used here for the approximation of $G(y)$.

The average displacement per hop μ is expected to increase with the electric field across the gate stack E_{ox}, as well as with the temperature T [36, 37]; the dependence of μ on E_{ox} and T is approximated by the expression

$$\mu(E_{ox}, T) = \mu_0 E_{ox}^m \exp\left(-\frac{\alpha E_{hop}}{k_{BT}}\right), \tag{4}$$

where $m \sim 2/3$ [37] and E_{hop} is the activation energy for the hopping of H^+ in the gate stack ($E_{hop} \sim 0.8$ eV for SiO_2).

The trapping of protons in the HfO_2 layer is modelled via the simple chemical reaction

$$Hf = O - Hf + H^+ \rightarrow [Hf = OH - Hf]^+, \tag{5}$$

leading to the following kinetic equation:

$$\frac{d}{dt}[Hf = OH - Hf]^+ = k_1[Hf = O - Hf][H^+] \tag{6}$$

where k_1 is the rate constant of equation (5) and $[H^+]$ is density of protons, calculated according to equation (3).

The simulated kinetics of defect generation, $N_{ox}(t)$, calculated according to equations (3) and (6), is shown in figure 10, for different values of the oxide electric field. The following

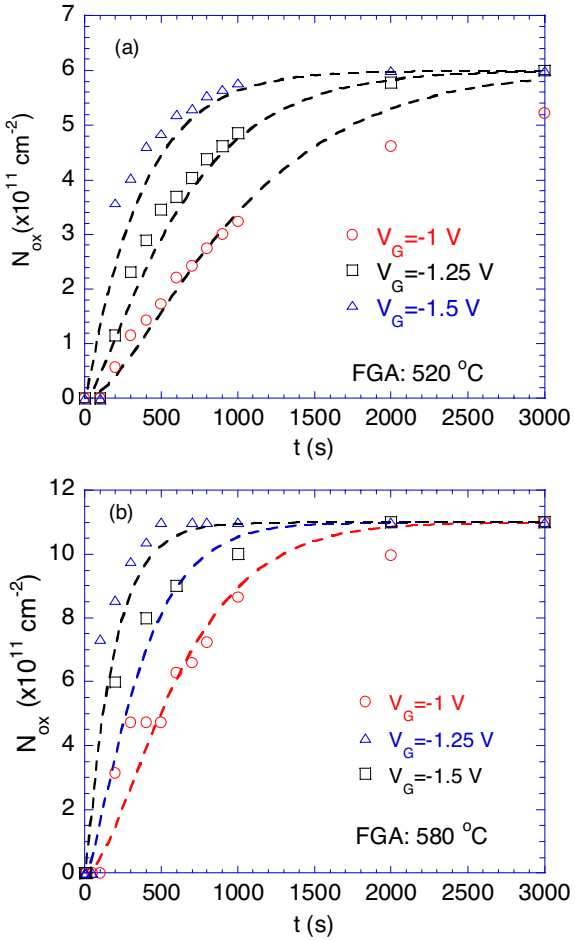

Figure 11. Effective density of positively charged defects as a function of time of pMOSFETs under NBT stress at different gate voltages, for devices exposed to FGA at 520 °C (a) and 580 °C (b). Symbols are experimental data and dashed curves are fits obtained using equations (3)–(6).

values of the physical parameters were fixed in the calculations: $t_{ox} = 5$ nm, $T = 400$ K, $\alpha = 0.3$ [37], $E_{hop} = 0.8$ eV and $k_1 = 3 \times 10^{-15}$ cm^2 s^{-1} [40]. One observes that N_{ox} increases rapidly with time, the more so when the oxide electric field increases, and reaches a saturation value; the saturation is reached when all the mobile protons are trapped at trivalent oxygen bridging centres in the HfO_2 layer. The relative increase of $N_{ox}(t)$ with E_{ox} comes from the increase of the average displacement per hop with the electric field, as given by equation (4).

The kinetics of the positive charge buildup during NBT stressing, extracted from the measured V_{th} shifts, is compared to the simulations in figures 11(a) and (b), for devices exposed to FGA at 520 and 580 °C, respectively. One observes that the model reproduces satisfactorily the time and voltage dependence of N_{ox}. The only free parameter used is the density of mobile protons transported away from the Si/SiO_2 interface, $[H_{interf}]$, which is equal to about 6×10^{11} and 1.1×10^{12} cm^{-2}, for devices annealed in FGA at 520 and 580 °C, respectively. The density of mobile protons in the gate stack is indeed expected to increase with the FGA temperature [41].

6. Conclusions

The role of hydrogen on the degradation of the electrical properties of MOS devices under negative bias temperature stress was discussed. The observed V_{th} shifts during NBT stressing were mainly caused by the buildup of positively charged defects in the gate stack. The positive charge was found (i) to increase with the forming gas annealing temperature of the device, (ii) to be robust under electron injection, (iii) to be partly removed by annealing the devices in N_2 at 200 °C. All these results indicated that hydrogen was most probably involved in the positive charge buildup. The kinetics of V_{th} shifts was then tentatively modelled by considering the trapping of protons in the HfO_2 layer. DFT calculations were first performed to investigate the stability of protons in monoclinic HfO_2. It was found that protons tend to bind to trivalent oxygen centres, forming overcoordinated defects. These defects were not producing any energetic level in the HfO_2 band gap, thus being robust against electron injection from the Si substrate. On the basis of these results, we developed a simple kinetic model for the positive charge buildup. When a negative bias was applied to the gate, interstitial protons present close to the Si/SiO_2 interface (resulting from the ionization of hydrogen atoms piled up at this interface) were transported dispersively towards the gate. Most of these protons were then assumed to be trapped at trivalent oxygen centres in the HfO_2 layer, forming stable positively charged overcoordinated defects, $[Hf = OH - Hf]^+$. The agreement between the simulations and experimental results was quite satisfactory; i.e. the model could explain the time and voltage dependence of the positive charge buildup, as well as the increased defect density observed when the temperature of the forming gas anneal of the device was increased.

Acknowledgments

Fruitful discussions with M Stoneham (University College London), A Pasquarello (Ecole Polytechnique Fédérale de Lausanne), A Edwards (Air Force Research Labs), G-M Rignanese and X Gonze (University of Louvain), V Afanas'ev (University of Leuven), J L Autran (University of Provence) and G Groeseneken (IMEC) are gratefully acknowledged. The authors are indebted to the IMEC High-k team for technical support. This work was financially supported by International Sematech and the IMEC Industrial Affiliation Program on High-k Dielectrics and Metal Gates.

References

[1] Van de Walle C G and Tuttle B R 2000 *IEEE Trans. Electron Devices* **47** 1779
[2] Brower K L 1988 *Phys. Rev.* B **38** 9657
Brower K L 1990 *Phys. Rev.* B **42** 3444
[3] Stesmans A 1996 *Appl. Phys. Lett.* **68** 2076
[4] Blöchl P E and Stathis J H 1999 *Phys. Rev. Lett.* **83** 372
[5] Pantelides S T, Rashkeev S N, Buczko R, Fleetwood D M and Schrimpf R D 2000 *IEEE Trans. Nucl. Sci.* **47** 2262
[6] Afanas'ev V V and Stesmans A 2001 *Europhys. Lett.* **53** 233
[7] Afanas'ev V V, Adriaenssens G J and Stesmans A 2001 *Micro. Eng.* **59** 85
[8] Warren W L, Vanheusden K, Fleetwood D M, Schwank J R, Shaneyfelt M R, Winokur P S and Devine R A B 1996 *IEEE Trans. Nucl. Sci.* **43** 2617
[9] Afanas'ev V V and Stesmans A 1998 *Phys. Rev. Lett.* **80** 5176
[10] For a recent review, see Houssa M (ed) 2004 *High-κ Gate Dielectrics* (London: Institute of Physics Publishing) and references therein
[11] Houssa M, Autran J L, Stesmans A and Heyns M M 2002 *Appl. Phys. Lett.* **709** 81
[12] Houssa M, Autran J L, Heyns M M and Stesmans A 2003 *Appl. Surf. Sci.* **212/213** 749

[13] Houssa M, Stesmans A, Carter R J and Heyns M M 2001 *Appl. Phys. Lett.* **78** 3289
[14] Houssa M, Afanas'ev V V, Stesmans A and Heyns M M 2001 *Semicond. Sci. Technol.* **16** L93
[15] Houssa M, Autran J L, Afanas'ev V V, Stesmans A and Heyns M M 2002 *J. Electrochem. Soc.* **149** F181
[16] Krishnan A T, Reddy V, Chakravarthi S, Rodriguez J, John S and Krishnan S 2003 *IEDM Technical Digest* (Piscataway, NJ: IEEE) p 349
[17] Helms C R and Poindexter E H 1994 *Rep. Prog. Phys.* **57** 791
[18] Ogawa S and Shiono N 1995 *Phys. Rev.* B **51** 4218
[19] Alam M A 2003 *IEDM Technical Digest* (Piscataway, NJ: IEEE) p 345
[20] Onishi K, Choi R, Kang C S, Cho H J, Kim Y H, Nieh R E, Han J H, Krishnan S A, Akbar M S and Lee J C 2003 *IEEE Trans. Electron Devices* **50** 1517
[21] Zhou X J, Rashkeev S N, Fleetwood D M, Schrimpf R D, Pantelides S T, Felix J A, Gusev E P and D'Emic C 2004 *Appl. Phys. Lett.* **84** 4394
[22] Zafar S, Lee B H, Stathis J H, Callegari A and Ning T 2004 *VLSI Symp.* (Piscataway, NJ: IEEE) p 208
[23] Onishi K, Kang C S, Choi R, Cho H J, Gopalan S, Nieh R E, Krishnan S A and Lee J C 2003 *IEEE Trans. Electron Devices* **50** 384
[24] Carter R J, Cartier E, Kerber A, Pantisano L, Schram T, De Gendt S and Heyns M M 2003 *Appl. Phys. Lett.* **83** 533
[25] Tsujikawa S, Mine T, Watanabe K, Shimamoto Y, Tsuchiya R, Ohnishi K, Onai T, Yugami J and Kimura S 2003 *Proceedings of the International Reliability Physics Symposium* (Piscataway, NJ: IEEE) p 183
[26] Nicollian E H and Brews J R 1982 *MOS Physics and Technology* (New York: Wiley)
[27] Afanas'ev V V and Stesmans A 1999 *J. Electrochem. Soc.* **146** 3409
[28] Chadi D J 2001 *Phys. Rev.* B **64** 195403
[29] Ordejón P, Artacho E and Soler J M 1996 *Phys. Rev.* B **53** R10441
[30] Soler J M, Artacho E, Gale J D, García A, Junquera J, Ordejón P and Sánchez-Portal D 2002 *J. Phys.: Condens. Matter* **14** 2745
[31] Balog M, Schrieber M, Michiman M and Patai S 1977 *Thin Solid Films* **42** 247
Aarik J, Aidla A, Mändar H, Sammelsberg V and Uustaer T 2000 *J. Cryst. Growth* **200** 105
[32] Russel R 1953 *J. Appl. Phys.* **24** 232
Wang J 1992 *J. Mater. Sci.* **27** 5397
[33] Kantorovich L N 1999 *Phys. Rev.* B **60** 15476
[34] Forster A S, Gejo F L, Shluger A L and Nieminen R M 2002 *Phys. Rev.* B **65** 174117
[35] Foster A S, Sulimov V B, Gejo F L, Shluger A L and Nieminen R M 2001 *Phys. Rev.* B **64** 224108
[36] McLean F B 1980 *IEEE Trans. Nucl. Sci.* **27** 1651
[37] Brown D B and Saks N S 1991 *J. Appl. Phys.* **70** 3734
[38] Devine N F M, Robertson J, Girault V and Devine R A B 2000 *Phys. Rev.* B **61** 15565
[39] McLean F B and Ausman G A 1977 *Phys. Rev.* B **15** 1052
[40] Houssa M, De Gendt S, Autran J L, Groeseneken G and Heyns M M 2004 *Appl. Phys. Lett.* **85** 2101
[41] Vanheusden K, Warren W L, Fleetwood D M, Schwank J R, Shaneyfelt M R, Draper B L, Devine R A B, Archer L B, Brown G A and Wallace R M 1998 *Appl. Phys. Lett.* **73** 674